*Revised manuscript with no changes marked

Chemosphere, Volume 247, May 2020, Article number 125799
DOI:10.1016/j.chemosphere.2019.125799

1 # Understanding the biochemical characteristics of struvite bio-
2 # mineralising microorganisms and their future in nutrient
3 # recovery

4 Yirong Leng, Robert Colston, Ana Soares*

5 Cranfield Water Science Institute, Cranfield University, Bedfordshire, MK43 0AL, UK

6 **Abstract**

7 The biochemical properties of selected microorganisms (*Bacillus pumilus,*
8 *Brevibacterium antiquum, Myxococcus xanthus, Halobacterium salinarum* and
9 *Idiomarina loihiensis*), known for their ability to produce struvite through
10 biomineralisation, were investigated. All five microorganisms grew at mesophilic
11 temperature ranges (22–34°C), produced urease (except *I. loihiensis*) and used bovine
12 serum albumin as a carbon source. *I. loihiensis* was characterised as a facultative
13 anaerobe able to use O_2 and NO_3 as an electron acceptor. A growth rate of 0.15 1/h was
14 estimated for *I. loihiensis* at pH 8.0 and NaCl 3.5% w/v. The growth rates for the other
15 microorganisms tested were 0.14-0.43 1/h at pH 7–7.3 and NaCl ≤1% w/v. All the
16 microorganisms produced struvite, as identified by morphological and X-ray Powder
17 Diffraction (XRD) analysis, under aerobic conditions. The biological struvite yield was
18 between 1.5–1.7 g/L of media, the ortho-phosphate removal and recovery were 55–76%
19 and 46–54%, respectively, the Mg^{2+} removal and recovery was 92–98% and 83–95%,

* Corresponding author at Cranfield Water Science Institute, Cranfield University,
Vincent Building, Cranfield, Bedfordshire, MK43 0AL, UK. Tel.: +44 (0) 1234 758121.
E-mail address: a.soares@cranfield.ac.uk.

Published by Elsevier. This is the Author Accepted Manuscript issued with: Creative Commons Attribution Non-Commercial No Derivatives License (CC:BY:NC:ND 4.0).
The final published version (version of record) is available online at DOI:10.1016/j.chemosphere.2019.125799. Please refer to any applicable publisher terms of use.

respectively. Large crystals (>300 μm) were observed, with coffin-lid and long-bar shapes being the dominant morphology of biological struvite crystals. The characterisation of the biochemical properties of the studied microorganisms is critical for reactor and process design, as well as operational conditions, to promote phosphorus recovery from waste streams.

Keywords: biomineral formation; struvite; biochemical properties; phosphorus recovery; statistical design

1 Introduction

Biological struvite (bio-struvite) has been identified as a route to recover phosphorus (P) from municipal wastewater streams (Soares et al., 2014). Microorganisms play an important role in struvite bio-mineralisation through different metabolic activities (Sinha et al., 2014) and by precipitation of specific structures or substances for microbial processes (Arias et al., 2017). Five microbial strains, *Halobacterium salinarum, Bacillus pumilus, Brevibacterium antiquum, Myxococcus xanthus,* and *Idiomarina loihiensis*, have been reported to be involved in biologically driven struvite formation in liquid streams (Table 1, González-Muñoz et al., 2008; Soares et al., 2014). *M. xanthus, I. loihiensis* and *H. salinarum* were reported to produce extracellular polymeric substances (EPS), which may fix cations and contribute to mineral heterogeneous nucleation and precipitation (González-Muñoz et al., 2010, 2008; Merroun et al., 2003). Most of the selected microorganisms can use O_2 as an electron acceptor (Table 1). *H. salinarum* has been reported to be able to use dimethyl sulfoxide

41 (DMSO) as an electron acceptor under anaerobic conditions, and use
42 photophosphorylation in the presence of light (Table 1).

43 *B. pumilus* and *M. xanthus* can use carbohydrates as a carbon source but this does not
44 apply to *B. antiquum* and *H. salinarum* According to the literature, all the selected
45 microorganisms can use protein/amino acids as a carbon source (Robinson, 2014;
46 Trujillo and Goodfellow, 2015). The utilisation of organic carbon sources depended on
47 enzyme production, and the rates of enzyme-catalysed reactions optimally performed
48 under appropriate temperature, pH and salinity ranges (Silva et al., 2016). The selected
49 microbial strains have been reported to grow in pHs from 5.5 to 9, and temperatures
50 ranging from 20–45 °C (Table 1). The halotolerant microorganisms *B. antiquum, H.*
51 *salinarum* and *I. loihiensis* can live in environments containing high NaCl (Gavrish et
52 al., 2004; González-Muñoz et al., 2008; Mesbah and Wiegel, 2005), particularly *H.*
53 *salinarum*, which can survive at extremely high NaCl concentrations (17.4~30.16 %,
54 Table 1).

55 Although some of the biochemical properties and growth conditions of selected
56 microorganism have been reported in the literature, some of the values are controversial
57 and further verification and characterisation is required. Statistical experimental design
58 is recognised as an approach widely used for parameter screening in optimisation
59 studies (Massey et al., 2009). By using such design, Simoes et al. (2017) investigated
60 the significant factors required for *B. antiquum* growth, and maximised the growth rates
61 in wastewater streams by screening and optimising a number of factors.

62 This study aims to investigate the biochemical properties of the selected
63 microorganisms owing to their capability to produce struvite through bio-
64 mineralisation. For industrial exploitation of microorganisms, the investigation of
65 biochemical characterisation is critical for appropriate processes design and meeting
66 microbial requirements by optimising reactor operational conditions. The temperature,
67 pH, electron acceptor, and organic carbon source are among the most important
68 environmental parameters affecting microbial growth and organic substance synthesis
69 (Silva et al., 2016). Knowledge of such parameters will allow the design of
70 reactors/processes and operational conditions to ensure proliferation of the selected
71 microorganisms, and even out-compete other microorganisms in mixed cultures, for
72 eventual enhanced P recovery by struvite from waste streams.

73 **Table 1 Biochemical properties of the five tested microorganisms**

		B. pumilus	*M. xanthus*	*B. antiquum*	*I. loihiensis*	*H. salinarum*
Strain		MTCC 1640	CECT 422	DSM 21545	MAH1 /CECT 5996	DSM 671
Type		Bacteria	Bacteria	Bacteria	Bacteria	Archaea
Gram reaction		+	-	+	-	-
Cell shape		Rod	Rod	Short rod/ coccoid	Rod	Rod
Size		0.6~0.7 x 2.0~3.0 µm	0.5 x 6 µm	0.6~1 µm	0.3~0.5 x 0.6–2 µm	0.5-1 x 1–6 µm
Motility		+	+	-	+	+
Endospore forming		+	+	-	-	-
O_2 requirement/tolerance		Aerobic	Aerobic	Aerobic	Aerobic	Facultative anaerobic, photophosphorylation at low O_2 concentration with light
Electron acceptor		O_2	O_2	O_2	O_2	O_2, dimethyl sulfoxide
Extracellular polymeric substances synthesis		Not documented	+	Not documented	+	+
Preferred organic carbon source	carbohydrate	Arabinose, mannitol, xylose, glucose, lactose, acetone	Glucose	Not able to directly use	Not documented	Not able to directly use
	protein/amino acid	Casein, lysine,	Amino acids	Casein, amino acid	Amino acid	Lysine, ornithine, arginine
	Other	Citrate, sucrose, D-trehalose, starch, D-glucose, D-arabinose, D-xylose, gelatin	Not documented	Gluconate, urea, gelatin, salicin, sorbitol	$_L$-alaninamide	Gelatin
Growth temperature		20~40 °C, optimum 30~35 °C	14~40°C, optimum 34~36°C	7°C, <37°C; optimum 24~26°C	2 ~ 43°C; optimum 28 ~37 °C	20~55°C, optimum 35~50°C
Growth pH		6~8, optimum at 7	5.5–9.0, optimum at 7	5.5~10, optimum at 7	not documented	5.5~8, optimum at 7
Growth in NaCl		0~2 %	not documented	0~18 %, optimum 3%	0.7~20 %, optimum 2~6 %	17.4~30.16 %, optimum 20.3 %
References		(Robinson, 2014; Shivaji et al., 2006)	(González-Muñoz et al., 2010; Janssen et al., 1977; Merroun et al., 2003; Poza et al., 2004; Robinson, 2014)	(Gavrish et al., 2004; Robinson, 2014; Simoes et al., 2017; Trujillo and Goodfellow, 2015)	(González-Muñoz et al., 2008)	(Losensky et al., 2017; Mesbah and Wiegel, 2005; Mormile et al., 2003; Zinder and Dworkin, 2013)

74 # 2 Material and methods

75 ## 2.1 Microbial strains and culture solution

76 Five microbial strains were used in this study: *H. salinarum* & *B. antiquum* (DSM 671
77 & DSM 21545, German Resource Centre for Biological Material, Germany), *B. pumilus*
78 (GB43, LGC Standards, Middlesex, UK), *M. xanthus* & *I. loihiensis* (CECT 422 &
79 MAH1 /CECT 5996, Spanish Type Culture Collection, University of Valencia, Paterna,
80 Spain). The microorganism were grown in synthetic B41 solution comprising 4 g/L
81 yeast extract, 2 g/L $MgSO_4 \cdot 7H_2O$ and 2 g/L K_2HPO_4 (Da Silva et al., 2000). The
82 solution was autoclaved at 121°C for 20 minutes and cooled to room temperature (20–
83 22°C). For inoculation of each microbial strain; 100 ml synthetic B41 solution in a 250
84 ml E-flask was inoculated with 0.9% w/v NaCl pre-washed pure cultures of the selected
85 microorganisms that were grown for 96 hours. The E-flasks were sealed with foam
86 stoppers and incubated on an orbital shaker (Stuart model SSL1, Fisher Scientific, UK)
87 at 150 rpm at room temperature. The halophile *I. loihiensis* was grown in B41 solution
88 with 1% w/v NaCl (González-Muñoz et al., 2008).

89 ## 2.2 Gram staining and enzyme production

90 Microorganisms, in their early exponential phase of growth (0-8 hours), were Gram-
91 stained using standard methods (Claus, 1992). A KB002™ HiAssorted Biochemical
92 Test Kit (HiMedia Laboratories Pvt. Ltd, India) was used to characterise the pure
93 cultures, according to the manufacturer's instructions. All tests were completed in
94 triplicate and a non-inoculated control was maintained under identical conditions.

95 2.3 **Statistical design of experiments**

96 To investigate the impact of growth conditions on microorganisms, a full factorial
97 experiment (FFD) was designed with five factors: temperature, initial pH, NaCl, Ca^{2+},
98 (by $CaCl_2$) and bovine serum albumin (BSA) as an additional carbon source (Table S1).
99 As factors that are key in optimising the industrial processes involving microbes (Silva
100 et al., 2016), additional variations in NaCl and Ca^{2+} were carried out as they have been
101 inferred to be detrimental to bacterial function and abiotic struvite growth (Le Corre et
102 al., 2005; Rivadeneyra et al., 2006). The tests were based upon low, medium and high
103 levels in relation to characterisation of municipal wastewater and sludge dewatering
104 liquors (Table S1). Temperatures varying from 6–34°C and pH 5.5–8.5 to cover the
105 range of temperatures and pH of municipal wastewater (Tchobanoglous et al., 2003). Ca
106 concentration was adjusted to 28 mg/L (Gassama et al., 2015). The NaCl content varied
107 between 0.5–3.5% w/v, based on characterisation of municipal wastewater and sludge
108 dewatering liquors in different full scale sites in the UK (Simoes et al 2017). (Table
109 S1).Three factors (temperature, NaCl and initial pH) at the 3-level and two factors (Ca^{2+}
110 and BSA) at the 2-level corresponded to $3^3 \times 2^2$ combinations of recipes, which were
111 studied in duplicate and thus generated $3^3 \times 2^2 \times 2 = 216$ tests for each microorganism.
112 The initial and final intact cell counts were examined to generate the overall cell
113 increase that was used as a response to the factors investigated. The experimental data
114 were fitted to a first-order linear regression model or second-order polynomial
115 regression model considering linear and quadratic forms of the independent factors. The
116 response surface methodology (RSM, (Bezerra et al., 2008)) was applied to examine the
117 significant relationship ($p<0.01$) between cell increase and the five growth factors, as

118 well as the significant two-factor interactions ($p<0.01$). The RSM was also used to
119 determine the optimal conditions that jointly maximise the cell increase by applying a
120 multiple response optimisation. All statistical design and analysis was performed using
121 Minitab 17 (Minitab, 2010).

122 ## 2.4 **Microbial cultivation under investigated growth conditions**

123 Microorganisms were grown in 96-well sterile microplates with working volume about
124 250 µl per well (Corning™, Fisher scientific, UK). Each well contained 234 µl solution
125 and 26 µl inoculum. To prepare the solutions corresponding to the FFD recipes (Table
126 S1), synthetic B41 solution with different NaCl concentrations was autoclaved and
127 mixed with 0.22 µm sterile filtered (Sartorius Stedim Biotech, Germany) BSA and
128 $CaCl_2$ concentrated solutions. The initial pH was adjusted by 0.1 M NaOH and 0.1 M
129 HCl sterile solutions. To minimise liquid evaporation from each well, only the central
130 wells (10 x 6) of the microplate were used for microbial inoculation, and the edge and
131 corner wells of the microplate were used for the non-inoculated controls (Syberg, 2016).
132 Breathable rayon film (VWR Collection, VWR, UK) was used to seal the microplates to
133 stop cross-contamination and to achieve uniform air and gas exchange, while also
134 reducing liquid evaporation for each well. The sealed microplates were then placed
135 inside a cube humidity chamber with four ventilation holes at each bottom corner and
136 with a water reservoir inside. The humidity chamber was kept at constant temperatures
137 of 6, 20 and 34 °C, incubated for 106, 66 and 48 hours, respectively. The application of
138 a humidity chamber was found to reduce liquid evaporation from 150 to 20–25 µl/well
139 by the end of the incubation period.

140 2.5 **Microbial cultivation at different dissolved oxygen levels**

141 After investigating microbial growth with the different FFD recipes, the conditions
142 that resulted in the highest increase of intact cell count were repeated but this time
143 ,incubation took at two dissolved oxygen (DO) levels using sacrificial glass vials. For
144 microbial cultivation under aerobic conditions, 30 ml sacrificial glass vials containing 9
145 ml synthetic B41 solution pre-adjusted in terms of pH, NaCl, Ca^{2+} and BSA were
146 inoculated with 1 ml inoculum and sealed with breathable film. The DO in the 30 mL
147 vials varied between 6–8 mg/L.

148 For microbial cultivation under anoxic/anaerobic conditions, synthetic B41 solution was
149 pre-adjusted in terms of pH, NaCl and bubbled with $N_{2(g)}$ after passing through a 0.22
150 µm sterile filter (Sartorius Stedim Biotech, Germany) at a rate of 30 L/min. The 10 ml
151 sacrificial glass vials were sealed with a nontoxic butyl rubber stopper and autoclaved
152 (121°C for 20 min). The DO in the 10 ml vials was close to 0 mg/L. Concentrated
153 solution of $CaCl_2$ and BSA, and 1 ml inoculum were then added using a sterile
154 disposable syringe and needle (VWR, UK). The capability of *I. loihiensis* to grow under
155 anoxic conditions was examined in synthetic solutions with absence of O_2 but with 0.5
156 g/L $NaNO_3$.

157 The glass vials were placed inside humidity chambers and incubated on an orbital
158 shaker-incubator (MAXQ5000 M6, Thermo Scientific, UK) at 150 rpm for 120 hours.
159 Samples were taken for examination at regular intervals (4–24 hours) through sacrificial
160 vials. All tests were completed in triplicate, and non-inoculated controls were
161 maintained under identical conditions.

162 2.6 **Abiotic struvite formation**

163 Abiotic struvite was prepared by mixing 200 mL 0.05 M $MgSO_4 \cdot 7H_2O$ with 100 ml 0.2
164 M $NH_4H_2PO_4$, both pre-adjusted to pH 9 with 1 M NaOH (Le Corre et al., 2005).
165 Concentrated BSA solution was added to the mixture at a rate of 4 g/L and incubated on
166 an orbital shaker at 150 rpm at room temperature for 24 hours.

167 2.7 **Crystal isolation, purification and determination**

168 The microorganisms were inoculated in 500 mL B41 media in sterile, 1 L Duran bottles,
169 sealed by a breathable film, and incubated under the investigated optimal growth
170 conditions at agitation rate 150 rpm for 120 hours. At the end of the incubation period,
171 the samples were filtered through a 10 μm nylon-mesh filter (Plastok, UK) and the
172 crystals were washed with deionised water twice. The isolated crystals were air-dried at
173 37°C for 2 hours and weighed to determine crystal yields. The pure crystals were then
174 identified by X-ray powder diffractometer (XRD, D5000, Siemens / Bruker, Germany).

175 2.8 **Analytical methods**

176 The intact cell count was examined by the SYBR Green I - propodium iodide co-
177 staining method using a flow cytometer (BD accuri C6, BD Biosciences, US, (Nocker et
178 al., 2017). Solution DO and pH values were determined with a portable DO- meter
179 (HQ40D, HACH, UK) and digital pH-meter (Jenway 3540, Bibby Scientific, UK). The
180 concentrations of soluble chemical oxygen demand (SCOD), PO_4-P, NH_4-N and NO_3-
181 N_2 were monitored with Merck Spectroquant® test kits. Mg^{2+} was measured by atomic
182 absorption spectroscopy (AAS, Analyst 800, PerkinElmer, UK) equipped with flaming

183 and electrothermal spectrometers. A high-resolution microscope (L-series upright
184 compound microscope, Division of GT vision Ltd, UK) was applied for observation of
185 Gram-stained cultures and crystal morphology in microbial cultures.

186 3 Results and discussion

187 3.1 **Microbial properties and enzyme production**

188 *B. pumilus* and *B. antiquum* were identified as Gram-positive and *M. xanthus, H.*
189 *salinarum* and *I. loihiensis* as Gram-negative, which agrees with previously published
190 information (Table 1). In particular, *B. pumilus* formed crusted two-cell clusters or
191 tetrads in B41 media, which were not observed in the other four microbial cultures.
192 Such cell structures did not grow in size but had the potential to aggregate together or
193 onto the crystal surface. Similar cell structures were observed as mineralised
194 *Thiomargarita* embryo-infesting cells (Bailey et al., 2007), and as silica spheroids onto
195 the cell sheath in microbial silicification (Yee et al., 2003). Thus, the crusted cell
196 structures observed during *B. pumilus* growth in this study is proposed associated with
197 the bio-mineralisation.

198 It is suggested that *B. pumilus* can form mineral particles along the cell surface during
199 exponential phase in solutions rich in PO_4-P and Mg^{2+}, and the mineral particles firmly
200 attach to the cell surface to form completely encrusted cell minerals. Based on previous
201 work on microbial mineralization occurring at the peptidoglycan wall due to negative
202 charges associated in gram-negative and gram-positive, concentrating cations such as
203 Mg^{2+} (Orange et al., 2009) and the consequential interaction with secreted phosphate

204 group and carboxyl groups which bind into the peptidoglycan framework of gram-
205 positive bacteria (Schultze-Lam et al., 1996).

206 The biochemical characterisation tests demonstrated varied enzyme production amongst
207 the microorganisms investigated. Nevertheless, it was quite remarkable to observe that
208 *H. salinarum*, *B. antiquum, B. pumilus* and *M. xanthus* were capable of using ornithine
209 as a carbon source and produced urease. Urease activity, as well as the degradation of
210 proteins, can generate energy for microbial growth and produce NH_3 as a by-product,
211 which raises the pH and release NH_4-N to combine with PO_4-P and Mg^{2+} for struvite
212 precipitation (Sadowski et al., 2014). Bio-mineralisation of struvite by urease-producing
213 microorganisms in the urinary tract has been reported, leading to the formation of
214 kidney stones, that typically contain 15–20% struvite (Arias et al., 2017; Coe et al.,
215 2005; Prywer and Torzewska, 2010).

216 *I. loihiensis* was the only microorganism investigated in this study that did not produce
217 urease and also the only one that showed a positive reaction of NO_3^- reduction to NO_2^-.
218 The latter is a common phenomenon in anoxic respiration, where NO_3^- was used as an
219 electron acceptor.

220 All five microorganisms showed neither positive nor negative results in terms of lysine
221 utilisation. They were also found to be negative for their ability to use citrate and
222 carbohydrates (including glucose, arabinose, lactose, adonitol and sorbitol) as a carbon
223 source, and for phenylalanine deamination and hydrogen sulfide production. The only
224 exception was that *B. pumilus* showed a 33% positive result for glucose utilisation. The

225 results obtained in this study partially agree with the organic carbon source utilisation
226 presented in Table 1.

227 3.2 **Identification of significant factors to microbial growth**

228 By applying the multi-response surface methodology, each microorganism was grown
229 in optimum conditions (Table 2) within the range of chemical conditions of wastewaters
230 and sludge dewatering liquors (Table S1). BSA was identified to have a significant
231 positive linear correlation ($p<0.01$) with microbial growth. All selected microorganisms
232 were able to use BSA as a carbon source (Table 2). Temperature, pH and NaCl were
233 also identified as being significant for microbial growth for all selected microorganisms.
234 A Ca^{2+} of 28 mg/L was identified to be required for growth of *I. loihiensis* but not for
235 *M. xanthus* growth, and was a non-significant factor for the other three microorganisms
236 (Table 2). In addition, temperature correlated with other factors (carbon source and p,
237 $p<0.01$) within the investigated range of 6-34°C. The growth of *B. pumilus, M. xanthus*,
238 and *I. loihiensis* had a positive linear correlation with the temperature and reached a
239 peak value at 34°C, while the relationship between temperature and cell count for *H.*
240 *salinarum* and *B. antiquum* fitted a quadratic trend and the growth peak occurred
241 between 22–24°C. Thus, the optimal growth temperature and enzyme activity for the
242 investigated microorganisms was within the mesophilic range of temperatures (Table 2).
243 Quadratic relationships between pH and microbial growth were also observed. *B.*
244 *pumilus, H. salinarum B. antiquum* and *M. xanthus* preferred neutral pH (7.1–7.3),
245 while *I. loihiensis* was observed to adapt to a mild alkaline pH of 8.0 (Table 2).
246 Furthermore, *I. loihiensis*, as a halophile, distinguished itself from the other four
247 microorganisms by its ability to adapt to grow at high NaCl concentration (3.5% w/v),

248 highlighting its ability to control the increased osmotic pressure due to higher salt
249 concentrations (Robinson, 2014). Whereas the other four microorganisms preferred a
250 reduced NaCl concentration (0.5–1% w/v, Table 2). A coefficient of determination (r^2)
251 was introduced to display the degree that the regression model approximates the real
252 data points, with an r^2 >0.7 typically being considered good (Grace-Martin, 2012). In
253 this study, the coefficient of determination was within the range of 0.71–0.94 (Table 2),
254 and thus the regression model could well explain the divergence of data points from a
255 trend.

256 **Table 2 Significant growth factors (main effect, p<0.01) and preferred growing conditions**
257 **defined by multi-response surface methodology**

	Temperature (°C)	NaCl (% w/v)	pH	BSA (g/L)	Ca^{2+} (mg/L)	r^2
B. pumilus	34	0.5	7.3	4	Ns	0.94
H. salinarum	24	0.5	7.1	4	Ns	0.80
B. antiquum	22	0.5	7.3	4	Ns	0.85
M. xanthus	34	1	7.2	4	0	0.73
I. loihiensis	34	3.5	8.0	4	28	0.71

258 Ns - Non-significant correlation to microbial growth

259 a – r^2, *ranging from 0 to 1, indicated the proportion of variation that can be explained*
260 *by the* regression model. r^2=1 indicates that the regression line perfectly fits the data.

261

262 ## 3.3 Microbial growth at different dissolved oxygen levels

263 No lag phase of microbial growth was observed under aerobic conditions (DO = 6-8
264 mg/L) and the exponential phase occurred within 24/48 hours of incubation starting.
265 The growth rates (μ) for the different microorganisms varied between 0.14 and 0.43

266 1/hour (Figure 1a). The relatively high growth rate of *B. pumilus* (0.35 1/hour) and *M.*
267 *xanthus* (0.24 1/hour) under anaerobic conditions distinguished themselves from the
268 other three microbial strains ($\mu \leq 0.04$ 1/hour, Figure 1a). The growth rate of *I. loihiensis*
269 under anoxic condition was 0.12 1/hour (Figure 1a), and >99.5% of NO_3-N was reduced
270 by the end of the incubation time. The final microbial intact cell counts for *B. pumilus,*
271 *B. antiquum*, *M. xanthus, H. salinarum, I. loihiensis* were 80–94% lower under
272 anaerobic conditions and 66% lower under anoxic conditions, than those under aerobic
273 conditions (Figure 1b). The SCOD removal was 20–27% under aerobic conditions, 0–
274 2.4% under anaerobic conditions. SCOD removal by *I. loihiensis* under anoxic
275 conditions was only *6%* (Figure 1c). Aerobic respiration, using O_2 as an electron
276 acceptor, is known to enable microorganisms to convert energy from carbon sources to
277 adenosine triphosphate production more efficiently than using other electron acceptors
278 (Kader & Saltveit, 2003). Hence, it was unsurprising that higher cell counts and SCOD
279 removal were observed under aerobic conditions (Figure 1b-c). None of the intact cell
280 microbial growth or SCOD removal was observed in non-inoculated controls.

281 *I. loihiensis* has been reported to be an aerobic organism (González-Muñoz et al., 2008).
282 However, in this study it was identified as a facultative anaerobe, able to use both O_2
283 and NO_3 as an electron acceptor. Although *B. pumilus* and *M. xanthus* have been
284 recognised as obligate aerobes (Robinson, 2014), in this study they were found to be
285 facultative anaerobes. There was no report related to *M. xanthus* being a facultative
286 anaerobe, although genome sequencing demonstrated that its common ancestor was a
287 facultative anaerobe (Thomas et al., 2008). Several *B. pumilus* strains have been
288 reported as facultative anaerobes, yet the electron acceptor has not been identified

289 (Alcaraz, 2015). *B. antiquum* was observed to be a strict aerobe in this study with a
290 specific growth rate of 0.14 1/hour, agreeing with previously reported growth rates in
291 wastewater with NaCl (3% w/v) and using acetate as the major carbon source
292 (equivalent to 1124 mg chemical oxygen demand/L, (Simoes et al., 2017)). Besides
293 carbon source and electron acceptor, exhaustion of macro/micro-nutrients (Maathuis,
294 2009) or formation of toxic metabolism by-products (Trinh and Srienc, 2009) cannot be
295 excluded as factors affecting the microbial growth.

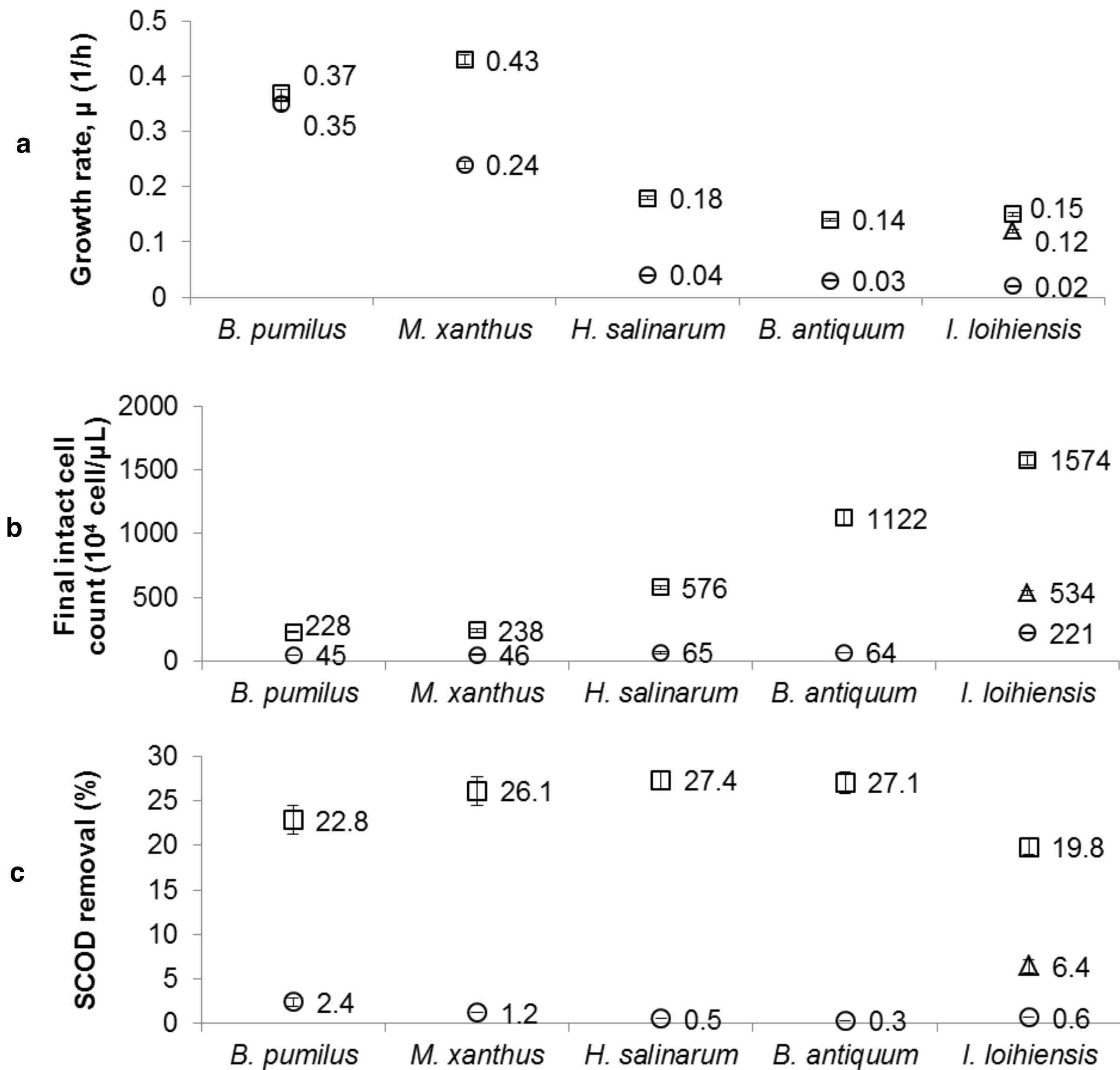

296 **Figure 1 Microbial growth rate (1/h) during exponential growth (0 - 24 /48 h) (a), and**
297 **intact cell counts (b) and SCOD removal (c). After 120 hour incubation period under**
298 **aerobic (□), anoxic (Δ) and anaerobic conditions (○). Error bars represent standard**
299 **deviation obtained from duplicates.**

3.4 **Identification of struvite crystals**

All the selected microorganisms produced crystals under aerobic conditions. The XRD diffractions results showed that the curves of isolated purified crystal products met the peak profile of the standard struvite crystals curve (pattern: COD 9007674). The crystals produced by all the microorganisms tested were hence identified as struvite (here called bio-struvite as it was formed through bio-mineralisation mechanism). The bio-struvite and the abiotic struvite crystals presented with the same dominant faces, with miller indices of [011], [111] and [00$\bar{1}$] (Table S2). Besides these three faces, [010] was also found predominant for the bio-struvite produced by *M. xanthus, H. salinarum, B. antiquum*, and *I. loihiensis* (Table S2).

The dominant morphology of the bio-struvite crystals was coffin-lid shape (Figure 2a-b, d-e) and long bar shape (Figure 2c), which have been reported to be among the most typical struvite forms (Tansel et al., 2018). The shape and size of these bio-struvite crystals were different from the relatively small dendritic abiotic struvite (Figure 2h). Abiotic struvite of such dendritic X-shape is typically formed at high pH ≥9 (Ronteltap et al., 2010; Ye et al., 2014). In most microbial cultures grown under aerobic conditions, crystals were observed as early as after 4 hours of incubation (Figure 2g) and these grew larger to more than 300 μm during stationary phase (Figure 2a-b, d-f). In *B. pumilus* culture, a considerable number of crusted tetrad clusters were observed aggregated on the specific bio-struvite crystal surface, particularly the [011] faces (Figure 2g). Bacteria (e.g. *Proteus mirabilis*) was reported to exert control on the bio-struvite crystal morphology (Torzewska et al., 2003). Prywer and Torzewska (2009) proposed a

322 potential of specific molecular interactions, which related the *P. mirabilis* capability of
323 binding to positively charged molecules (e.g. $Mg[H_2O]_6^{2+}$ octahedra) in the crystal
324 surface structure. Such molecular interactions varied with the composition of the
325 microbial secreted biomolecules (e.g. polysaccharide) and its affinity for cations
326 (Prywer and Torzewska, 2009), as well as the charged molecules' type and density on
327 the crystal surface (Sadowski et al., 2014). In this study, the microbial growth may have
328 potential to enhance specific faces of the bio-struvite crystals (e.g. [011], [111], $[00\bar{1}]$
329 miller indices) and therefore lead to the different crystal morphology (e.g. coffin-lid
330 shape).

331 The self-assembly of crystals such as contact twinning (Figure 2i-j) and penetration
332 twining (Figure 2k) were observed, along with the parallel grouping of coffin-lid shaped
333 crystals (Figure 2l) and long-bar shaped crystals (Figure 2m). Some bio-struvite crystals
334 were observed with truncated apices, which was related to enhanced [111] end caps
335 (Figure 2n). Similar struvite crystals were observed at low or moderate pH (8–8.5,
336 (Sadowski et al., 2014)).

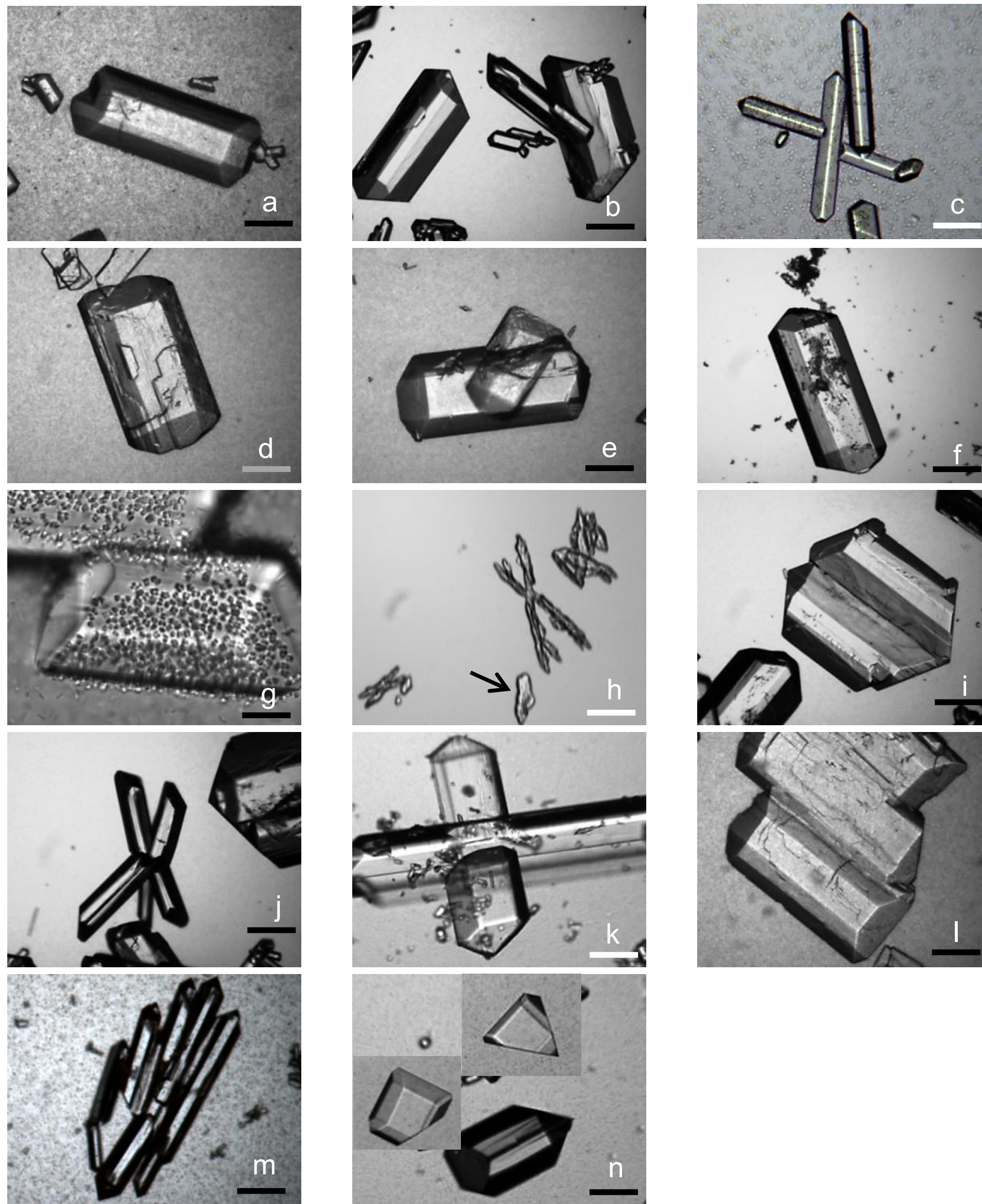

337 **Figure 2 Coffin-lid and long-bar shaped bio-struvite produced in stationary phase by (a) -**
338 ***B. pumilus;* (b, c) - *M. xanthus;* (d) - *H. salinarum;* (e) - *B. antiquum* and (f) - *I. loihiensis*.**
339 **(g) Crusted cell cluster aggregated on *B. pumilus* bio-struvite crystal surface (4 h**
340 **incubation); (h) - dendritic abiotic struvite crystals, bio-struvite crystals contact twinning**
341 **(i-k), parallel grouping (l-m), bio-struvite crystals with truncated apices (n), Black bar**
342 **scale – 88.32 µm, white bar scale – 35.93 µm, grey bar scale – 10.19 µm.**

343 3.5 **Removal and recovery of ortho-phosphate and magnesium**

344 The bio-struvite crystal yields under aerobic conditions varied between 1521 and 1746
345 mg crystals per litre synthetic solution (Table 3). No crystal was collected under
346 oxygen-limiting conditions (Table 3). The removal of PO_4-P and Mg^{2+} by the end of the
347 120 hour incubation time varied with DO levels. Under aerated conditions, the removal
348 of PO_4-P and Mg^{2+} was between 55–76% and 92–98%, respectively. Under anaerobic
349 conditions, the removal of PO_4-P and Mg^{2+} varied between 1–2% and 2–8% of Mg^{2+},
350 respectively. Under anoxic conditions, *I. loihiensis* was able to remove 2% of PO_4-P
351 and 32% of Mg^{2+}, from the synthetic media (Table 3).

352 A mass balance to the nutrients in solution (liquid and crystals <10 μm) demonstrated
353 that considerable amounts of PO_4-P and Mg^{2+} recovered were as bio-struvite (46–54%
354 and 83–95%, respectively (Table 3). Although *B. antiquum* removed a relatively high
355 content of PO_4-P (314 mg/L, 76%) from the synthetic solution, the PO_4-P recovery
356 (48%) by bio-struvite crystals was lower than those for *B. pumilus*, *M. xanthus* and *H.*
357 *salinarum* (52–54%). Moreover, the Mg^{2+} recovery by *B. antiquum* (84%) and *I.*
358 *loihiensis* (83%) was observed to be lower than for the other three microorganisms (92–
359 95%).

360 **Table 3 Removal and recovery of PO_4-P and Mg^{2+} at two DO levels by the end of 120 hour**
361 **incubation period.**

	DO (mg/L)	Bio-struvite [a] production (mg bio-struvite/L synthetic solution)	PO_4-P removal	Mg^{2+} removal	PO_4-P recovered by bio-struvite [a]	Mg^{2+} recovered by bio-struvite [a]
B. pumilus	7.2	1700	265 ± 3 mg/L 64%	176 ±1 mg/L 98%	215 mg/L 52%	167 mg/L 93%
	0	0	8 ± 3 mg/L 2%	5 ± 1 mg/L 2%	-	-
M. xanthus	7.2	1746	272 ± 1 mg/L 66%	177 ± 0 mg/L 98%	221 mg/L 54%	171mg/L 95%
	0	0	5 ± 1 mg/L 1%	9 ± 1 mg/L 5%	-	-
H. salinarum	7.8	1692	276 ± 1 mg/L 67%	170 ± 0 mg/L 94%	215 mg/L 52%	166 mg/L 92%
	0	0	7 ± 0 mg/L 2%	7 ± 1 mg/L 4%	-	-
B. antiquum	8.0	1550	314 ± 1 mg/L 76%	173 ± 0 mg/L 96%	196 mg/L 48%	152 mg/L 84%
	0	0	7 ± 3 mg/L 1%	10 ±1 mg/L 6%	-	-
I. loihiensis	6.2	1521	229 ± 1 mg/L 55%	166 ±0 mg/L 92%	192 mg/L 46%	149 mg/L 83%
	0	0	4 ± 2 mg/L 1%	14 ±5 mg/L 8%	-	-
	0[b]	0	9 ± 3 mg/L 2%	58 ±1 mg/L 32%	-	-
control	-	0	0	0	-	-

362 a - Bio-struvite crystals >10 µm

363 b - Anoxic condition with 0.5 g/L $NaNO_3$

364 The synthesis of bio-struvite and removal of PO_4-P and of Mg^{2+} have been reported to
365 depend on microbial growth and metabolism pathways (Sinha et al., 2014). The significant
366 difference of PO_4-P removal and bio-struvite crystal yields between aerobic and anaerobic
367 conditions in this study indicates the importance of DO for P removal and bio-struvite
368 production. Furthermore, the capability of the selected microorganisms, particularly *I.*
369 *loihiensis,* to produce bio-struvite and remove PO_4-P in this study might be underestimated
370 due to the NaCl concentration of 3.5% w/v. It was reported that the increased NaCl could
371 increase the solubility of the struvite phase and therefore lead to inhibition of the bio-struvite
372 crystal size (Rivadeneyra et al., 2006). Significant prevention of bio-struvite production was
373 also observed on sludge dewatering liquors with 3% w/v NaCl (Simoes et al., 2017). The
374 molar ratio of the removed PO_4-P to Mg^{2+} by *B. antiquum* under aerobic conditions ([PO_4-
375 P]/[Mg^{2+}] =1.4) was relatively higher than the standard stoichiometric ratio [PO_4-P]/[Mg^{2+}]
376 of struvite, indicating that *B. antiquum* may absorb considerable amounts of PO_4-P into cells.
377 Such PO_4-P accumulation within *B. antiquum* cells was reported to be relative to the
378 formation of intracellular bio-struvite (Smirnov et al., 2005).

379 *M. xanthus* displayed a higher recovery rate of bio-struvite, in comparison with the other
380 microbial strains investigated. Although it removes less P than other strains (66% compared
381 to 76% by *B. antiquum*) less of the resource was lost inside biomass or as small crystals.
382 Furthermore, *M. xanthus* presented high growth rates (0.43 1/h) and competitive SCOD
383 removal among the others tested (Figure 1). On the other side, its final intact cell count was
384 amongst the lowest, indicating it may be more susceptible to changing conditions
385 experienced in a batch reactor.

386 3.6 **Implication to the wastewater industry**

387 Similar to most biological processes in conventional wastewater treatment, bio-struvite
388 production will be ideally applied in open, mixed-culture conditions. The microorganisms
389 enrolled in bio-struvite production are required to out-compete others and become the
390 dominant species in a mixed-microbial culture. The investigation of microbial capabilities
391 and growth of the selected microorganisms in this study can help identify the suitable types
392 of streams (e.g. municipal wastewater, urine, addition of seawater to wastewater) for optimal
393 resource recovery. Streamline reactor and process design, with the most appropriate
394 operational conditions regarding temperature, pH, availability of certain nutrients, and
395 concentrations of NaCl, Ca^{2+} and DO (Table 2). By tailoring processes based on these results
396 the chance for the selected bio-struvite-producing bacteria out-competing other microbial
397 communities in wastewaters increases, whilst efficiency controlling the system can reduce
398 energy and additive costs.

399 The findings of biochemical characterisation in this study (

400 Table 4) can be compared with existing information (Table 1). This study's findings indicate
401 that *B. pumilus, M. xanthus, B. antiquum* and *H. salinarum* have the potential to grow in urine
402 due to their ability to produce urease and adapt to lower pH (urine pH 5-7), suggesting that
403 these bacterium would be viable options for urine-separated stream treatment and resource
404 recovery. This also has the benefit of reducing the uncertainty of these bacteria being out
405 competed by mixed-cultures in wastewaters, as urine in typically sterile, improving
406 decentralised system's efficiency and reliability. *I. loihiensis* has the ability to grow under
407 anoxic conditions, alkaline pH, high concentrations of NaCl and Ca^{2+} (e.g. seawater) and can
408 possibly be used in selective chemical pressures for competitive growth. *B. pumilus, M.*
409 *xanthus* and *I. loihiensis* have the potential to grow in effluents from mesophilic digesters of
410 temperature around 35 °C. Furthermore, specific wastewater streams characterised by high
411 load of protein/amino acids (e.g. dairy processing wastewater) are proposed as preferred
412 wastewater sources to grow the microorganisms. In all scenarios a well-aerated environment
413 was identified as being essential for bio-struvite production, which can be achieved by pre-
414 existing infrastructure in wastewater treatment plants as secondary treatment process are
415 aerobic, with forced or passive aeration (Tchobanoglous et al., 2003).

416 With the increased knowledge in struvite recovery, researchers have also been investigating
417 its suitability as a fertiliser. This study has shown that bio-struvite produces coffin-lid shaped,
418 tabular crystals, whilst abiotic struvite produced was more dendritic crystal morphologies
419 (Figure 2). The abiotic struvite produced conformed to other studies, where pH exceeded 9
420 (Ronteltap et al., 2010; Ye et al., 2014). The crystal morphologies of bio-struvite (Figure 2)
421 have been demonstrated more suitable for direct land application, as the reduced surface area

422 from more euhedral crystals, improving its soil retention time as a fertiliser (Shaddel et al.,
423 2019.

424 **Table 4 Summary of biochemical properties of investigated microorganisms and comparison**
425 **with existing literature (based on Table 1)**

	New	Agreement
Enzyme production	• *B. pumilus, M. xanthus* and *H. salinarum* produce urease	• *B. antiquum* produce urease
Electron acceptor	• *I. loihiensis* – O_2 and NO_3-N (facultative anaerobe) • *B. pumilus* and *M. xanthus* are facultative anaerobes [c]	• All the tested microorganism can use O_2 as electron acceptor [a]
Carbon source	• *I. loihiensis* cannot directly use carbohydrates, but can use proteins • *B. pumilus* and *M. xanthus* cannot directly use carbohydrates [b, c]	• *B. antiquum, I. loihiensis* and *H. salinarum* cannot directly use carbohydrates • *B. pumilus, M. xanthus, H. salinarum* and *B. antiquum* can use amino acids/proteins
Growth temperature	• *H. salinarum* prefer mesophilic temperature (24°C) [c]	• *B. pumilus M. xanthus* and *I. loihiensis* prefer high mesophilic temperature (34°C) • *B. antiquum* prefer mesophilic temperature (22°C)
Growth pH	• *I. loihiensis* can grow within pH 5.5–8.5, and prefer mild alkaline pH 8	• *B. pumilus, M. xanthus, B. antiquum* and *H. salinarum* prefer neutral pH (7.1–7.3)
Growth NaCl	• *M. xanthus* prefer 1% w/v NaCl • *B. antiquum* and *H. salinarum* prefer 0.5% w/v NaCl [c]	• *I. loihiensis* prefer 3.5% w/v NaCl • *B. pumilus* prefer 0.5 % w/v NaCl
Growth Ca^{2+}	• Positive effect of Ca^{2+} of 28 mg/L on *I. loihiensis* growth • Negative effect of Ca^{2+} of 28 mg/L on *M. xanthus* growth	

426 a - Microorganisms produced bio-struvite only under aerobic conditions.
427 b - The *B. pumilus* were 33% positive for glucose utilisation.
428 c – Different findings from previous studies.

429 # 4 Conclusion

430 • Proteins/amino acids were the preferred organic carbon sources for the five
431 microorganisms investigated.
432 • *B. pumilus, M. xanthus, H. salinarum* and *B. antiquum* were able to produce urease.
433 • *I. loihiensis* was found to be a facultative anaerobe able to use O_2 and NO_3-N as an
434 electron acceptor.
435 • The preferred temperature for all selected microorganisms was within the mesophilic
436 range (22–34 °C); most microorganisms preferred a neutral pH and NaCl concentrations
437 less than 1% w/v, whereas *I. loihiensis* preferred a mild alkaline pH 8, high NaCl of 3.5%
438 w/v and the presence of Ca^{2+}.
439 • The selected microorganisms produced bio-struvite crystals under aerobic conditions. The
440 morphology of crystals produced was dominantly coffin-lid and long-bar shapes.
441 • The bio-struvite production and PO_4-P removal highly depended on the microbial growth
442 and DO level. At the investigated optimal growing conditions, in the presence of DO, the
443 bio-struvite crystal (>10 μm) yield and PO_4-P removal varied between 1,521–1,746 mg/L
444 and 55–76%, respectively.
445

446 # 5 Reference

447 Alcaraz, G., 2015. Gisella Alcaraz Bacillus Pumilus [WWW Document]. URL
448 https://microbewiki.kenyon.edu/index.php/Gisella_Alcaraz-Bacillus_Pumilus (accessed
449 1.1.19).

450 Arias, D., Cisternas, L., Rivas, M., 2017. Biomineralization mediated by ureolytic bacteria

451 applied to water treatment: a review. Crystals 7, 345.
452 https://doi.org/10.3390/cryst7110345

453 Bailey, J. V., Joye, S.B., Kalanetra, K.M., Flood, B.E., Corsetti, F.A., 2007. Evidence of
454 giant sulphur bacteria in Neoproterozoic phosphorites. Nature 445, 198–201.
455 https://doi.org/10.1038/nature05457

456 Bezerra, M.A., Santelli, R.E., Oliveira, E.P., Villar, L.S., Escaleira, L.A., 2008. Response
457 surface methodology (RSM) as a tool for optimization in analytical chemistry. Talanta
458 76, 965–977. https://doi.org/10.1016/j.talanta.2008.05.019

459 Claus, D., 1992. A standardized Gram staining procedure. World J. Microbiol. Biotechnol. 8,
460 451–452. https://doi.org/10.1007/BF01198764

461 Coe, F.L., Evan, A., Worcester, E., 2005. Kidney stone disease. J. Clin. Invest. 115, 2598–
462 2608. https://doi.org/10.1172/JCI26662.2598

463 Da Silva, S., Bernet, N., Delgenès, J.P., Moletta, R., 2000. Effect of culture conditions on the
464 formation of struvite by Myxococcus xanthus. Chemosphere 40, 1289–1296.
465 https://doi.org/10.1016/S0045-6535(99)00224-6

466 Gassama, U.M., Puteh, A. Bin, Abd-Halim, M.R., Kargbo, B., 2015. Influence of municipal
467 wastewater on rice seed germination, seedling performance, nutrient Uptake, and
468 chlorophyll content. J. Crop Sci. Biotechnol. 18, 9–19. https://doi.org/10.1007/s12892-
469 014-0091-4

470 Gavrish, E.I., Krauzova, V.I., Potekhina, N. V, Karasev, S.G., Plotnikova, E.G., Altyntseva,
471 O. V, Korosteleva, L. a, Evtushenko, L.I., 2004. Three new species of brevibacteria,
472 Brevibacterium antiquum sp. nov., Brevibacterium aurantiacum sp. nov. and

473 Brevibacterium permense sp. nov. Microbiology 73, 218–225.
474 https://doi.org/10.1023/B:MICI.0000023986.52066.1e

475 González-Muñoz, M.T., De Linares, C., Martínez-Ruiz, F., Morcillo, F., Martín-Ramos, D.,
476 Arias, J.M., 2008. Ca-Mg kutnahorite and struvite production by Idiomarina strains at
477 modern seawater salinities. Chemosphere 72, 465–472.
478 https://doi.org/10.1016/j.chemosphere.2008.02.010

479 González-Muñoz, M.T., Rodriguez-Navarro, C., Martinez-Ruiz, F., Arias, J.M., Merroun,
480 M.L., Rodriguez-Gallego, M., 2010. Bacterial biomineralization: new insights from
481 Myxococcus-induced mineral precipitation. Geol. Soc. London, Spec. Publ. 336, 31–50.
482 https://doi.org/10.1144/SP336.3

483 Grace-Martin, K., 2012. Can a regression model with a small R-squared be useful? [WWW
484 Document]. Anal. Factor. URL http://www.theanalysisfactor.com/small-r-squared/
485 (accessed 2.1.19).

486 Janssen, G.R., Wireman, J.W., Dworkin, M., 1977. Effect of temperature the growth of
487 Myxococcus xanthus. J. Bacteriol. 130, 561–562.

488 Le Corre, K.S., Valsami-Jones, E., Hobbs, P., Parsons, S. a., 2005. Impact of calcium on
489 struvite crystal size, shape and purity. J. Cryst. Growth 283, 514–522.
490 https://doi.org/10.1016/j.jcrysgro.2005.06.012

491 Leng, Y. and Soares, A. (2018) Understanding the fundementals of bio-struvite
492 biomineralization in wastewater, Cranfield University. PhD thesis, in review

493 Losensky, G., Jung, K., Urlaub, H., Pfeifer, F., Fröls, S., Lenz, C., 2017. Shedding light on
494 biofilm formation of Halobacterium salinarum R1 by SWATH-LC/MS/MS analysis of

495 planktonic and sessile cells. Proteomics 17, 1–13.
496 https://doi.org/10.1002/pmic.201600111

497 Maathuis, F.J., 2009. Physiological functions of mineral macronutrients. Curr. Opin. Plant
498 Biol. 12, 250–258. https://doi.org/10.1016/j.pbi.2009.04.003

499 Massey, M.S., Davis, J.G., Ippolito, J.A., Sheffield, R.E., 2009. Effectiveness of recovered
500 magnesium phosphates as fertilizers in neutral and slightly alkaline soils. Agron. J. 101,
501 323–329. https://doi.org/10.2134/agronj2008.0144

502 Merroun, M.L., Chekroun, K. Ben, Arias, J.M., González-Muñoz, M.T., 2003. Lanthanum
503 fixation by Myxococcus xanthus: Cellular location and extracellular polysaccharide
504 observation. Chemosphere 52, 113–120. https://doi.org/10.1016/S0045-6535(03)00220-
505 0

506 Mesbah, N., Wiegel, J., 2005. Halophilic thermophiles: A novel group of extremophiles, in:
507 Microbial Diversity: Current Perspectives and Potential Applications. IK Publishing
508 House, New Delhi, pp. 91–118.

509 Minitab, 2010. Minitab 17 Statistical Software.

510 Mormile, M.R., Biesen, M.A., Gutierrez, M.C., Ventosa, A., Pavlovich, J.B., Onstott, T.C.,
511 Fredrickson, J.K., 2003. Isolation of Halobacterium salinarum retrieved directly from
512 halite brine inclusions. Environ. Microbiol. 5, 1094–1102.
513 https://doi.org/10.1046/j.1462-2920.2003.00509.x

514 Nocker, A., Cheswick, R., Dutheil de la Rochere, P.M., Denis, M., Léziart, T., Jarvis, P.,
515 2017. When are bacteria dead? A step towards interpreting flow cytometry profiles after
516 chlorine disinfection and membrane integrity staining. Environ. Technol. 38, 891–900.

517 https://doi.org/10.1080/09593330.2016.1262463

518 Orange, F., Westall, F., Disnar, J.R., Prieur, D., Bienvenu, N., Le Romancer, M., DÉfarge, C.,
519 2009. Experimental silicification of the extremophilic Archaea Pyrococcus abyssi and
520 Methanocaldococcus jannaschii: applications in the search for evidence of life in early
521 Earth and extraterrestrial rocks. Geobiology 7, 403–418. https://doi.org/10.1111/j.1472-
522 4669.2009.00212.x

523 Poza, M., Sieiro, C., Villa, T.G., 2004. Cloning and expression of clt genes encoding milk-
524 clotting proteases from Myxococcus xanthus 422. Appl. Environ. Microbiol. 70, 1–6.
525 https://doi.org/10.1128/AEM.70.10.6337

526 Prywer, J., Torzewska, A., 2010. Biomineralization of struvite crystals by Proteus mirabilis
527 from artificial urine and their mesoscopic structure. Cryst. Res. Technol. 45, 1283–1289.
528 https://doi.org/10.1002/crat.201000344

529 Prywer, J., Torzewska, A., 2009. Bacterially induced struvite growth from synthetic urine:
530 experimental and theoretical characterization of crystal morphology. Cryst. Growth Des.
531 9, 3538–3543. https://doi.org/10.1021/cg900281g

532 Rivadeneyra, M.A., Delgado, R., Párraga, J., Ramos-Cormenzana, A., Delgado, G., 2006.
533 Precipitation of minerals by 22 species of moderately halophilic bacteria in artificial
534 marine salts media: Influence of salt concentration. Folia Microbiol. (Praha). 51, 445–
535 453. https://doi.org/10.1007/BF02931589

536 Robinson, R.K., 2014. Encyclopaedia of food microbiology (1st ed.), Academic press.

537 Ronteltap, M., Maurer, M., Hausherr, R., Gujer, W., 2010. Struvite precipitation from urine -
538 Influencing factors on particle size. Water Res. 44, 2038–2046.

539 https://doi.org/10.1016/j.watres.2009.12.015

540 Sadowski, R.R., Prywer, J., Torzewska, A., 2014. Morphology of struvite crystals as an
541 evidence of bacteria mediated growth. Cryst. Res. Technol. 49, 478–489.
542 https://doi.org/10.1002/crat.201400080

543 Schultze-Lam, S., Fortin, D., Davis, B., Beveridge, T., 1996. Mineralization of bacterial
544 surfaces. Chem. Geol. 132, 171–181. https://doi.org/10.1016/S0009-2541(96)00053-8

545 Shaddel, S., Ucar, S., Andreassen, J., Sterhus, S., 2019 Engineering of struvite crystals by
546 regulating supersaturation- Correlation with phosphorus recovery, crystal, morphology
547 and process efficiency. J. Environ. Chem. Eng. Elsevier Ltd, 7(1).
548 https://doi.org/10.1016/j.jece.2019.102918

549 Shivaji, S., Chaturvedi, P., Suresh, K., Reddy, G.S.N., Dutt, C.B.S., Wainwright, M.,
550 Narlikar, J. V., Bhargava, P.M., 2006. Bacillus aerius sp. nov., Bacillus aerophilus sp.
551 nov., Bacillus stratosphericus sp. nov. and Bacillus altitudinis sp. nov., isolated from
552 cryogenic tubes used for collecting air samples from high altitudes. Int. J. Syst. Evol.
553 Microbiol. 56, 1465–1473. https://doi.org/10.1099/ijs.0.64029-0

554 Silva, T. Da, Cássia, V. De, Amanda Lais de Souza Coto, Rafael de Carvalho Souza,
555 M.B.S.N., Gomes, E., Bonilla-Rodriguez, G.O., 2016. Effect of pH, temperature, and
556 chemicals on the endoglucanases and β-glucosidases from the thermophilic fungus
557 Myceliophthora heterothallica F.2.1.4. obtained by solid-state and submerged cultivation.
558 Biochem. Res. Int. 2016. https://doi.org/10.1155/2016/9781216

559 Simoes, F., Vale, P., Stephenson, T., Soares, A., 2017. Understanding the growth of the bio-
560 struvite production Brevibacterium antiquum in sludge liquors. Environ. Technol. 1–10.

561 https://doi.org/10.1080/09593330.2017.1411399

562 Sinha, A., Singh, A., Kumar, S., Khare, S.K., Ramanan, A., 2014. Microbial mineralization
563 of struvite: a promising process to overcome phosphate sequestering crisis. Water Res.
564 54, 33–43. https://doi.org/10.1016/j.watres.2014.01.039

565 Smirnov, A., Suzina, N., Chudinova, N., Kulakovskaya, T., Kulaev, I., 2005. Formation of
566 insoluble magnesium phosphates during growth of the archaea Halorubrum distributum
567 and Halobacterium salinarium and the bacterium Brevibacterium antiquum. FEMS
568 Microbiol. Ecol. 52, 129–137. https://doi.org/10.1016/j.femsec.2004.10.012

569 Soares, A., Veesam, M., Simoes, F., Wood, E., Parsons, S. a., Stephenson, T., 2014. Bio-
570 Struvite: A new route to recover phosphorus from wastewater. Clean - Soil, Air, Water
571 42, 994–997. https://doi.org/10.1002/clen.201300287

572 Syberg, S., 2016. Reducing the edge effect in cell culture microplates [WWW Document].
573 Thermo Fish. Sci. URL https://www.rdmag.com/article/2016/10/reducing-edge-effect-
574 cell-culture-microplates (accessed 2.1.19).

575 Tansel, B., Lunn, G., Monje, O., 2018. Struvite formation and decomposition characteristics
576 for ammonia and phosphorus recovery: A review of magnesium-ammonia-phosphate
577 https://doi.org/10.1016/j.chemosphere.2017.12.004

578 Tchobanoglous, G., Burton, F.L., Stensel, H.D., Metcalf&Eddy, 2003. Wastewater
579 engineering: Treatment and reuse, 4th ed. McGraw-Hill Education.

580 Thomas, S.H., Wagner, R.D., Arakaki, A.K., Skolnick, J., Kirby, J.R., Shimkets, L.J.,
581 Sanford, R.A., Löffler, F.E., 2008. The mosaic genome of Anaeromyxobacter
582 dehalogenans strain 2CP-C suggests an aerobic common ancestor to the delta-

583 proteobacteria. PLoS One 3. https://doi.org/10.1371/journal.pone.0002103

584 Torzewska, A., Stączek, P., Rózalski, A., 2003. Crystallization of urine mineral components
585 may depend on the chemical nature of Proteus endotoxin polysaccharides. J. Med.
586 Microbiol. 52, 471–477. https://doi.org/10.1099/jmm.0.05161-0

587 Trinh, C.T., Srienc, F., 2009. Metabolic engineering of Escherichia coli for efficient
588 conversion of glycerol to ethanol. Appl. Environ. Microbiol. 75, 6696–6705.
589 https://doi.org/10.1128/AEM.00670-09

590 Trujillo, M.E., Goodfellow, M., 2015. Brevibacterium, in: Bergey's Manual of Systematics of
591 Archaea and Bacteria. John Wiley & Sons, Inc., in association with Bergey's Manual
592 Trust, pp. 1–22. https://doi.org/10.1002/9781118960608.gbm00062

593 Ye, Z., Shen, Y., Ye, X., Zhang, Z., Chen, S., Shi, J., 2014. Phosphorus recovery from
594 wastewater by struvite crystallization: Property of aggregates. J. Environ. Sci. 26, 991–
595 1000. https://doi.org/10.1016/S1001-0742(13)60536-7

596 Yee, N., Phoenix, V.R., Konhauser, K.O., Benning, L.G., Ferris, F.G., 2003. The effect of
597 cyanobacteria on silica precipitation at neutral pH: Implications for bacterial
598 silicification in geothermal hot springs. Chem. Geol. 199, 83–90.
599 https://doi.org/10.1016/S0009-2541(03)00120-7

600 Zinder, S.H., Dworkin, M., 2013. Morphological and physiological diversity, in: The
601 Prokaryotes: Prokaryotic Biology and Symbiotic Associations. Springer New York, pp.
602 185–220. https://doi.org/10.1007/978-3-642-30194-0_9